Impact of Shunt Resistance on the Assessment of Multijunction I-V

Iván Lombardero[a)] and Carlos Algora

Instituto de Energía Solar, Universidad Politécnica de Madrid, Madrid, Spain

[a)]Corresponding author: ivan.lombardero@ies.upm.es

Abstract. Simple but powerful rules of thumb, derived from the electrical equivalent circuit of single junction solar cells, are usually applied to understand artifacts in solar cell measurements. However, this can mislead to wrong diagnosis in multijunction solar cells, especially when shunt resistances are involved. Thus, it is important to specify which artifacts can be caused by shunt resistances in a multijunction solar cell. Moreover, as the shunt resistance impact on monojunction solar cells is related to the low voltage operation region, there is a lack of studies regarding its impact on *FF* or V_{OC} operation points for multijunction solar cells. In this work we point out the differences between the shunt resistance impact in multijunction and single junction solar cell I-V curves under illumination conditions.

INTRODUCTION

Electric models have been widely used to simulate and understand the performance of solar cells[1-3]. These models simulate the solar cell performance as a set of electronic devices such as diodes, current sources and resistances. The well-known electric circuit model for the monojunction solar cell leads straight forward to relate each device of the model to a given effect in the I-V curve including measurement artifacts. These connections between measurement artifacts and the devices of the model are part of the common wisdom, as single junction solar cells (Si, CdTe, GaAs, etc.) broadly dominate PV applications and their model is very simple. However, applying the rules of thumb of the monojunction model to multijunction measurements may provide erroneous conclusions thus, misleading in the detection of new material weaknesses, manufacture yield issues, or on-field degradation detection.

To the best of our knowledge, in multijunction solar cells only the impact of the shunt resistance in quantum efficiency measurements has been thoroughly studied[4-6]. Recently, there have been some efforts pointing out the impact of the shunt resistance close to V_{OC} conditions in GaAs/GaAs tandem solar cells[7]. Nevertheless, there is no study analyzing the impact of the shunt resistance in concentrator triple junction solar cells under real operation conditions. Understanding the real effects of the shunt resistance in the I-V curve is especially important since many failures detected in concentrator solar cells are attributed to a decrease in the shunt resistance[8]. We will show that, under illumination conditions, low shunt resistances in a given subcell, can resemble the I-V curve of a solar cell with an increase in ohmic losses and recombination currents. Moreover, *FF* evolution as a function of concentration can be deceiving, making necessary to apply other characterization techniques to provide an accurate interpretation of the measurements under illumination. Accordingly, this work is mainly devoted to point out which artifacts of the I-V curve under illumination are caused by low shunt resistances in multijunction solar cells.

MONOJUNCTION VS. MULTIJUNCTION ARTIFACTS

Approach

Distributed circuits models have been widely used to simulate the solar cell performance and their accuracy have been extensively proved[1-3]. The model used in this work is a three-dimensional distributed circuit. It is made up of

14th International Conference on Concentrator Photovoltaic Systems (CPV-14)
AIP Conf. Proc. 2012, 060001-1–060001-6; https://doi.org/10.1063/1.5053525
Published by AIP Publishing. 978-0-7354-1728-1/$30.00

different electronic circuits related to unit cells representing the front solar cell surface (active area, metal or perimeter). For the sake of simplicity only the model of the monojunction solar cell is shown in Fig.1.a. The electric model of the triple junction solar cell connects more subcells vertically (i.e. a set of diodes, current sources and a shunt resistance) together with vertical and horizontal resistances. Each tunnel junction between two subcells has been simulated as a simple vertical resistance, as they have been proved to stand outstanding density currents without leaving its ohmic performance range[9-10]. Each unit cell is concatenated and connected to the contiguous ones (through the lateral resistances) in order to build up a circuit equivalent to the whole solar cell. The simulated solar cell is a GaInP/Ga(In)As/Ge standard triple junction with a 5.5x5.5 mm^2 area and a comb-like metal grid (Fig.1.b) with an efficiency of 40% at 500×. These parameters have been chosen since they are the most common in the current CPV industry.

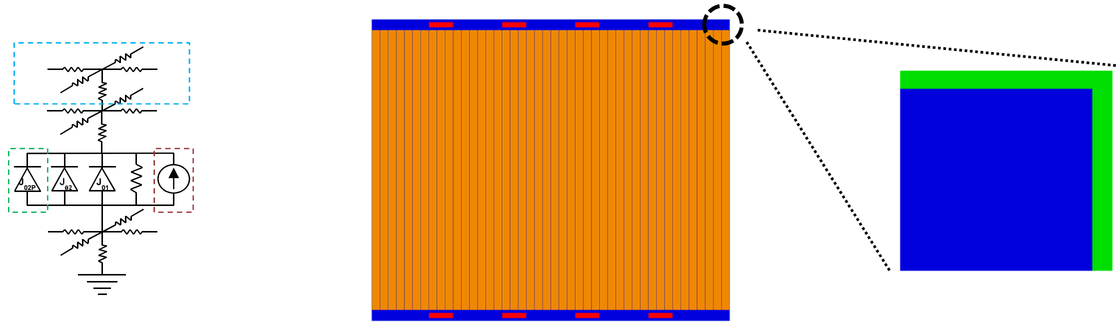

(a) (b) (c)

FIGURE 1. Layout of the model used to carry out the simulations: a) Monojunction solar cell equivalent circuit, the characteristic devices of each circuit (illuminated, metal or perimeter) have been highlighted (orange, blue and green respectively). b) Front view of the simulated solar cell: active area is shown in orange, metal in blue, wires in red and perimeter in green c) Magnification of the perimeter region.

Shunt Resistance Impact on the Solar Cell Performance

In order to evaluate the impact of the shunt resistance, the whole area of each subcell in the 3J solar cell has been shunted independently. A GaInP single junction solar cell (with the same parameters as those of the GaInP top subcell of the 3J) has also been shunted for comparison (Fig.2). I-V curve dependence on the diode and the series resistance parameters are also evaluated to show which monojunction rules of thumb can be applied to multijunction solar cells.

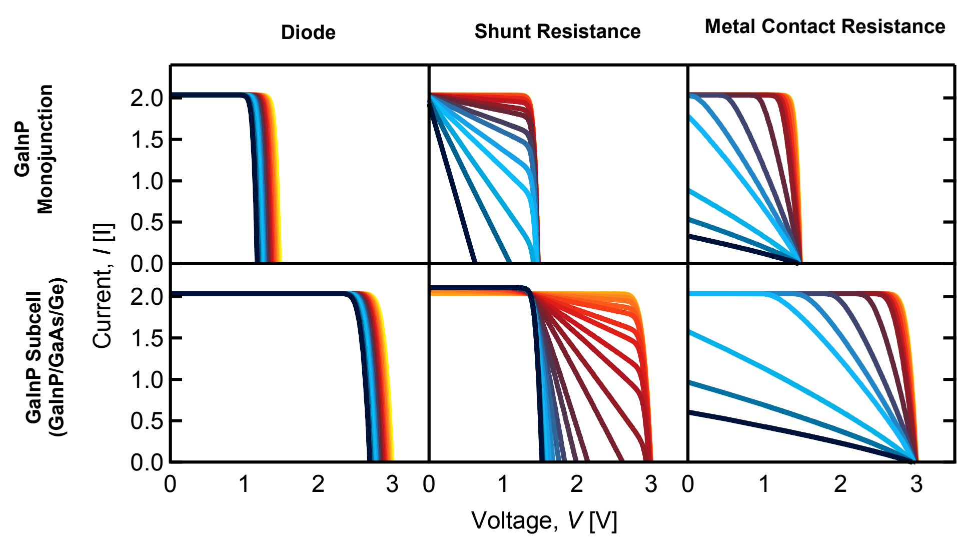

FIGURE 2. Diode, shunt resistance and series resistance degradation applied on a GaInP monojunction and on a GaInP subcell in a 3J solar cell. The GaInP subcell was set as the limiting current subcell.

Rules of Thumb Comparison

The monojunction rules of thumb (Fig.2) related to each device of the equivalent circuit used to evaluate the effects appearing in the solar cell I-V shape are:

- *Higher diode saturation current → Lower V_{OC}*
  Diodes are used to simulate recombination currents at different regions of the solar cell (neutral region, space charge region or perimeter). Increasing their saturation currents increases the recombination currents, thus decreasing the open circuit voltage. The other main diode parameter is the diode ideality factor whose variation is not considered in this paper (only fixed values of 1and 2 are used) as this will only be a mathematical approximation without any physical meaning behind it. Alternative ideality factors (such as 2/3 for Auger recombination[11]) might be used in a more advanced model. Nevertheless, this will not affect the main results of this paper since the diode ideality factor only changes the main voltage range of impact of a diode but not the way it changes the I-V curve shape.
- *Higher series resistance → Lower slope at open circuit voltage conditions*
  There are different series resistances inside the solar cell (semiconductor or metal, horizontal or vertical, etc.). Therefore, each type of series resistance may have different impacts on other properties (such as the electroluminescence for instance) but all of them can be understood as a loss of voltage on the I-V curve, decreasing the slope at V_{OC}.
- *Lower shunt resistance → Higher slope at I_{SC} operation point*
  Shunt resistances are used to simulate leakage currents through the p-n junction at the bulk or at the perimeter. The lower the shunt resistance the higher the leakage current, thus increasing the slope at 0 V.

Now, if we compare these rules of thumb with the effects observed in the 3J solar cell we find:

- *Higher saturation currents of the diodes → Lower Voc (same as monojunction)*
- *Higher series resistance → Lower slope at open circuit voltage condition (same as monojunction)*
- *Lower shunt resistance for one subcell → Different impacts depending on the shunting level*

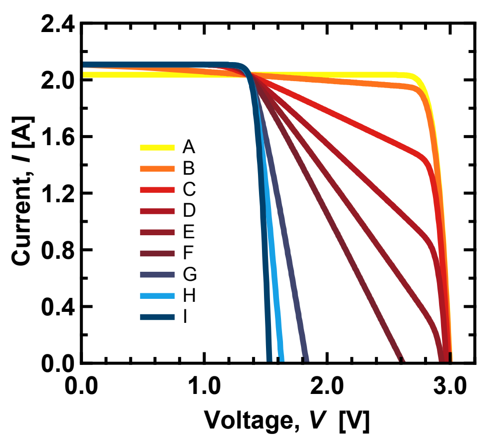

FIGURE 3. 3J solar cell with different shunt resistances in the top subcell (which was the limiting one before being shunted).

I-V curve as a function of the top subcell shunt resistance, has been plotted in Fig.3 to highlight the most important scenarios (curve A shows the standard non-degraded 3J solar cell I-V). As the shunt resistance decreases, an extra slope appears for voltages higher than the non-shunted subcells V_{OC}, decreasing the *FF* (curves B, C and D). For even lower shunt resistance values the "new" slope starts to affect lower currents approaching V_{OC} operation point (curve E) until the shunt is seen as a straight line between the sum of the other (non-shunted) subcells V_{OC}'s and the 3J V_{OC}. At this point, the slope created by the shunt dominates the high voltage region instead of the series resistance (in the absence of very high series resistance losses). Therefore, the slope at V_{OC} is determined by the shunt, so that the slope is directly related to the difference between the 3J V_{OC} and the sum of the non-shunted subcells V_{OC}'s. The higher the difference between them the smallest the slope created by the shunt. In this situation the multijunction I-V would resemble that one of a solar cell with high ohmic losses (low slope at V_{OC}). If the shunt keeps decreasing, the multijunction V_{OC} will decrease as well, while the *FF* will recover, resembling the I-V curve of a 3J with low ohmic losses (in the absence of high series resistances) and high recombination currents (curves F,G,H). This is due to the fact that all the 3J solar cell voltage loss caused by the shunt is lost in the shunted subcell. Therefore, the ratio between the 3J V_{OC} and the sum of V_{OC}'s of the non-shunted subcells approaches unity as the shunt resistance decreases, increasing the *FF* as well as the slope at V_{OC} as the 3J V_{OC} decreases. Finally, V_{OC} and *FF* becomes those of the two non-shunted subcells (curve I). Another effect that could be observed is an increase in the 3J I_{SC} if the shunted subcell was the limiting one before being shunted[7] (curves B to I). When the 3J is at 0 V, the shunted subcell will be biased at negative voltages by the other subcells, promoting its current generation increase (as it is shunted). It is especially important to keep this in mind since the characterization of high concentrator solar cells is usually quite challenging. The achievement of spectral matching conditions at high irradiation levels for all subcells is very complex, so that this current increase could be misunderstood as incorrect measurements conditions (i.e. non-spectral matched).

Therefore, we can summarize the shunt resistance impact of a subcell in the multijunction solar cell in three scenarios:

1. Several slopes before P_{MAX} and I_{SC} increase (if limiting subcell gets shunted)
   Shunt resistance can be easily diagnosed at this shunt levels
2. Slope at V_{OC} determined by the shunt resistance
   I-V shape resembles series resistance losses
3. V_{OC} lost and *FF* recovery
   I-V shape turns to resemble lower series resistance losses and higher current recombination losses as the shunt resistance decreases

Once the impact of the shunt resistance in the multijunction solar cell has been pointed out, the influence of illumination is analyzed. First we analyzed the influence of different illumination ratios (shunted subcell respect to non-shunted ones) in the impact of the subcell shunt on the multijunction I-V performance. Secondly we assess the evolution of the *FF* and V_{OC} of a multijunction solar cell with a shunted subcell as the overall illumination increases.

Over/Undercurrent Generation Influence on the Impact of the Shunt Resistance on the I-V

Perfect spectral matching conditions (i.e. all subcells generate exactly the same current) are not the case for most situations. Even if the subcells are perfectly adjusted to generate the same current (which are not in a standard triple junction due to Germanium subcell overcurrent), spectrum variations will change the current generation distribution between the subcells. Only space solar cells could be spectrum matched in the long term, as the extraterrestrial spectrum is much more constant and stable. Photogeneration ratios between subcells change the impact of shunting a given subcell in the multijunction performance. On the one hand, if a subcell generates less current than the other ones, its effect will always impact the multijunction I-V. Moreover, as previously pointed out, an increase in the I_{SC} will be observed if the limiting subcell gets shunted. On the other hand, if a subcell that generates more current than the other ones get shunted (for instance the Germanium subcell in a standard 3J), its effect will not be observed until the shunt affects current levels under the I_{SC} of the other subcells. Additionally, its effect will not be seen at voltages close to the sum of the V_{OC}'s of the non-shunted subcells as aforementioned, but at voltages close to the sum of the V_{OC} of the non-shunted subcells and the voltage at which the I-V curve of the shunted subcell generates such a low current as the other two subcells. Therefore, shunts in overgenerating subcells are especially deceiving as their impact is observed later than expected, and once they become noticeable, the slope created by the shunt is high. Therefore, it is easier to think of a series resistance as the root cause of this effect instead of a shunt resistance

This is particularly important regarding the standard 3J solar cell where the Germanium subcell usually generates almost twice current as the two upper subcells, thus making the Germanium subcell more insensitive to shunts and decreasing its impact on the overall power generation. Additionally, industry is moving forward four or more junctions, which has the direct impact of halving the current generated by the Germanium subcell and thus increasing the artifact caused by its shunt (if any). This means that Germanium subcell shunts will have a higher impact on the multijunction performance for 4 junction solar cells than for the standard triple one, thus being necessary to reevaluate its reliability and its impact in the overall performance.

Shunt Impact as a Function of the Shunted Subcell Concentration

FF empirical formulas[12] are used to predict *FF* evolution as a function of the concentration taking into account the effect of the shunt resistance. However, they are useful only for monojunction solar cells as they only take the shunt effect to decrease the *FF* by a given factor. Nevertheless, a multijunction solar cell *FF* follows a more complex trend, decreasing and increasing as concentration increases (see Fig.4). We can distinguish five ranges:

1. At the beginning the multijunction solar cell does not have any voltage contribution from the shunted subcell and it has a better fill factor than if it would not have a shunted subcell.
2. The shunted subcell starts to increase its voltage contribution, but at the cost of decreasing the fill factor of the multijunction solar cell.
3. Once the overall voltage of the shunted solar cell starts to achieve the one of the non-shunted solar cell, *FF* stops decreasing and starts to recover.
4. When current generation is high enough, shunt resistance effect disappears, thus *FF* and the V_{OC} become the same of the non-shunted solar cell.
5. Finally, the series resistance dominates the solar cell performance making the FF decrease again.

Those concentrations at which the solar cell V_{OC} is close to the non-shunted one but still has a low *FF* are especially deceiving. As its shape will resemble that of a solar cell with semiconductor and series resistance degradation. Moreover, for some concentration levels increasing the concentration will reduce fill factor, showing a similar behavior to that of a series limited solar cell. Therefore, wide concentration ranges need to be analyzed to distinguish between shunt and series resistances. Otherwise other characterization techniques are needed, what is now ongoing work in our group.

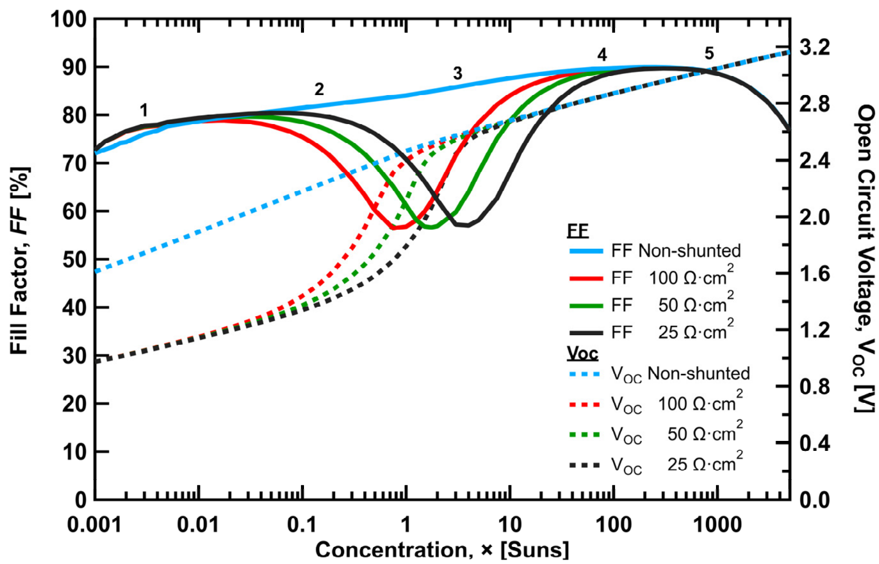

FIGURE 4. *FF* and V_{OC} evolution as a function of the concentration for a 3J solar cell with a shunted middle subcell (for three different values of the shunt) and a standard 3J solar cell (no subcells shunted) for comparison. Each number pints out one range of the FF evolution.

CONCLUSIONS

The impact of the shunt resistance in 3J solar cells has been analyzed and compared to the rules of thumb of single junction solar cells. We have shown that for low shunt resistances the I-V shape resembles that of a single junction solar cell with high series resistance and high recombination currents. The influence of the illumination on the impact of the shunt resistance in the subcell in the I-V features has been assessed as well, pointing out the higher impact that will have low shunt resistances in germanium subcells for architectures with more than three junctions.

ACKNOWLEDGMENTS

This work has been supported by the Spanish MINECO through the project PCIN-2015-181-C02-02 (acronym DINAMIC of the SOLAR-ERANET program) and by the Comunidad de Madrid through the project MADRID-PV (S2013/MAE-2780). I. Lombardero is funded by the Spanish MINECO through an FPU14. V. Orlando are acknowledged for providing the solar cells which motivated this paper.

REFERENCES

1. B. Galiana, C. Algora, I. Rey-Stolle, and I. Vara, "A 3-D Model for Concentrator Solar Cells Based on Distributed Circuit Units," *IEEE Trans. Electron Devices*, vol. 52, no. 12, pp. 2552–2558, Dec. 2005.
2. P. Espinet, I. García, I. Rey-Stolle, C. Algora, and M. Baudrit, "Extended description of tunnel junctions for distributed modeling of concentrator multi-junction solar cells," *Sol. Energy Mater. Sol. Cells*, vol. 95, no. 9, pp. 2693–2697, Sep. 2011.
3. P. Espinet, C. Algora, J. R. González, N. Núnez, and M. Vázquez, "Degradation mechanism analysis in temperature stress tests on III–V ultra-high concentrator solar cells using a 3D distributed model," *Microelectron. Reliab.*, vol. 50, no. 9–11, pp. 1875–1879, Sep. 2010.
4. E. Barrigón, P. Espinet-González, Y. Contreras, and I. Rey-Stolle, "Implications of low breakdown voltage of component subcells on external quantum efficiency measurements of multijunction solar cells," *Prog. Photovoltaics Res. Appl.*, vol. 20, no. 1, pp. 6–11, 2012.
5. M. Meusel, C. Baur, G. Létay, A. W. Bett, W. Warta, and E. Fernandez, "Spectral response measurements of monolithic GaInP/Ga(In)As/Ge triple-junction solar cells: Measurement artifacts and their explanation," *Prog. Photovoltaics Res. Appl.*, vol. 11, no. 8, pp. 499–514, 2003.
6. J.-J. Li, S. H. Lim, C. R. Allen, D. Ding, and Y.-H. Zhang, "Combined Effects of Shunt and Luminescence Coupling on External Quantum Efficiency Measurements of Multijunction Solar Cells," *IEEE J. Photovoltaics*, vol. 1, no. 2, pp. 225–230, Oct. 2011.
7. F. Oviedo, Z. Liu, Z. Ren, M. Thway, T. Buonassisi, and I. M. Peters, "Ohmic shunts in two-terminal dual-junction solar cells with current mismatch," *Jpn. J. Appl. Phys.*, vol. 56, p. 08MA05, 2017.
8. V. Orlando, M. Gabás, B. Galiana, P. Espinet-González, S. Palanco, N. Nuñez, M. Vázquez, K. Araki, and C. Algora, "Failure analysis on lattice matched GaInP/Ga(In)As/Ge commercial concentrator solar cells after temperature accelerated life tests," *Prog. Photovolt Res. Appl.*, 2016.
9. E. Barrigón, I. García, L. Barrutia, I. Rey-Stolle, and C. Algora, "Highly conductive p + + -AlGaAs/n + + -GaInP tunnel junctions for ultra-high concentrator solar cells," *Prog. Photovoltaics Res. Appl.*, vol. 22, no. 4, pp. 399–404, Apr. 2014.
10. I. García, I. Rey-Stolle, and C. Algora, "Performance analysis of AlGaAs/GaAs tunnel junctions for ultra-high concentration photovoltaics," *J. Phys. D. Appl. Phys.*, vol. 45, no. 4, p. 45101, 2012.
11. P. Espinet-González, I. Rey-Stolle, M. Ochoa, C. Algora, I. García, and E. Barrigón, "Analysis of perimeter recombination in the subcells of GaInP/GaAs/Ge triple-junction solar cells," *Prog. Photovoltaics Res. Appl.*, vol. 23, no. 7, pp. 874–882, Jul. 2015.
12. M. A. Green, "Solar cell fill factors: General graph and empirical expressions," Solid State Electron., vol. 24, no. 8, pp. 788–789, 1981.